Periodic intensity distribution (PID) of mica polytypes: symbolism, structural model orientation and axial settings

Massimo Nespolo,[a]*† Hiroshi Takeda,[b] Toshihiro Kogure[a] and Giovanni Ferraris[c]

[a]*Mineralogical Institute, Graduate School of Science, University of Tokyo, 7-3-1 Hongo, Bunkyo-ku, Tokyo 113-0033, Japan,* [b]*Research Institute, Chiba Institute of Technology, 2-17-1 Tsudanuma, Narashino, Chiba 275-0016, Japan, and* [c]*Department of Mineralogical and Petrologic Sciences, University of Torino, via Valperga Caluso 35, 10125 Torino, Italy. E-mail: nespolo@nirim.go.jp*

Abstract

Following a preliminary revisitation of the nomenclatures in use for mica polytypes, the properties of the periodic intensity distribution (PID) function, which represents the Fourier transform of the stacking sequence, are analysed. On the basis of the relative rotations of neighbouring layers, mica polytypes are classified into three types; for each type, the PID exists in different subspaces of the reciprocal space. A revised procedure to compute the PID, in which further restrictions on the structural model orientation are introduced, is presented. A unifying terminology based upon the most common symbols used to describe mica polytypes (RTW, Z and TS) is derived; these symbols represent the geometrical basis for the computation of the PID. Results are presented for up to four layer polytypes and are compared with the reflection conditions derived by means of Zvyagin's functions. Both the PID values and the reflection conditions are expressed in suitable axial settings and compared with previous partial reports, revealing some errors in previous analyses. A computer program to compute PID from the stacking symbols is available.

1. Introduction

Micas are phyllosilicates with general formula $IM_{2-3}T_4O_{10}A_2$ (Rieder *et al.*, 1998) (*I*: interlayer cations; *M*: octahedral cations; *T*: tetrahedral cations; *A* = O, OH, F, Cl). They are built by stacking a 2:1 or *T–O–T* (tetrahedral–octahedral–tetrahedral) layer (Figs. 1 and 2) with interlayer cations between adjacent layers. The *T–O–T* layer is commonly considered as a cleavage unit (Kogure, 1997) and polytypism arises from the stacking of this layer with $n \times 60°$ rotations ($0 \leq n \leq 5$) (Smith & Yoder, 1956). Polytypes in which the position of any layer relative to the others and the transition from it to the adjacent layers are the same or equivalent for all

layers are called homogeneous polytypes (Zvyagin, 1988). The homogeneous polytypes were first derived by Smith & Yoder (1956), who called them 'simple polymorphs'. By using Ramsdell (1947) notation, these polytypes are identified as $1M, 2M_1, 3T, 2M_2, 2O$ and $6H$ [symbols according to Guinier *et al.* (1984)]. On the basis of the symmetry of the *O* sheet, homogeneous polytypes have been divided into three families of MDO (maximum degree of order) polytypes (Backhaus & Ďurovič, 1984; see below).

Several authors have used different symbols and approaches to deal with the problem of identifying the stacking sequence of mica polytypes. The most relevant results have been published in different journals and languages during the past forty years; therefore, they are briefly summarized below. The most powerful tool for unravelling the stacking sequence appears to be the comparison between the observed and calculated values of the periodic intensity distribution (PID) function.
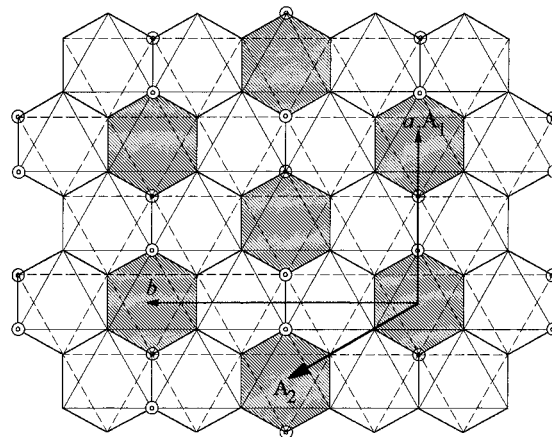

Fig. 1. The octahedral sheet of micas shown in (001) projection. The *M*1 sites are shaded, *M*2 sites are not shaded; concentric circles indicate OH/F groups. A_1 and A_2 are hexagonal axes: they are rotated 30° clockwise from the orientation given by Sadanaga & Takeda (1969) and Takeda & Sadanaga (1969). *a* and *b* are orthohexagonal axes, traced according to the standard orientation for Z symbols (Zhukhlistov *et al.*, 1990); they correspond to the orthohexagonal cell C_1 as defined by Arnold (1996).

---

† Present address: National Institute for Research in Inorganic Materials, Research Center for Creating New Materials, 1-1 Namiki, Tsukuba-shi, Ibaraki 305-0044, Japan.

This is the Fourier transform of the stacking sequence, obtained by removing the modulating effect of the layer transform from the structure factor (Takeda, 1967; Sadanaga & Takeda, 1969; Takeda & Sadanaga, 1969; Takeda & Ross, 1995; see below). Hereinafter, the conditions under which PID can be obtained are revised, the computation procedure is redefined and a general correlation among the symbols involved is derived.

Hexagonal axes in the plane of the layer are henceforth indicated as (A_1, A_2), whereas orthohexagonal axes are represented as (a, b). Diffraction indices expressed in hexagonal axes are written as upper-case letters $(HK.L)$, whereas those expressed in orthohexagonal or monoclinic axes are written as lower-case letters (hkl). The orientation of the (a, b) axes with respect to (A_1, A_2) is that between the orthohexagonal C_1 cell and the hexagonal P cell [see the work of Arnold (1996) and Nespolo, Takeda & Ferraris (1997) and Nespolo et al. (1998)].†

1.1. Choice of the unit layers

Following Takéuchi (1971) and Takéuchi & Haga (1971), the T–O–T layer is henceforth called the M layer. Three translationally independent cationic sites exist in the O sheet. One site is *trans*-coordinated by OH/F and is labelled $M1$; when the layer is centrosymmetric, the centre of symmetry is at this site. The remaining two sites are *cis*-coordinated by OH/F and are labelled $M2$; when the layer contains a symmetry plane, this plane relates the two $M2$ sites (Fig. 1). Depending on the occupation of the M sites, micas are divided into tri-octahedral and di-octahedral types. Then, on the basis of the distribution of the cations in these sites, the symmetry of the octahedral sheet can be $H(\bar{3})12/m$ (homo-octahedral: the three sites are occupied by the same cation), $P(\bar{3})12/m$ (meso-octahedral: one site is occupied by a cation different from that in the other two sites) or $P(3)12$ (hetero-octahedral: all the three sites are differently occupied) (Ďurovič, 1994a) [layer-group notation after Dornberger-Schiff (1959), details given by Merlino (1990)]. In the so-called Pauling model (Pauling, 1930), the T sheets have layer symmetry $P(6)mm$. In the real structure, because of the difference in the lateral dimensions of the T and O sheets, tetrahedra rotate around $\mathbf{c}^*$ (Takéuchi & Sadanaga, 1959) and the degree of rotation depends mainly upon the chemical composition and the temperature (Takeda & Mori, 1970; Takeda & Morosin, 1975; Catti et al., 1989). The model that takes into account this rotation is hereinafter called the trigonal model. The trigonal model is also known as the Radoslovich model (Rado-

slovich, 1961). It was proposed for the first time by Belov (1949). The tetrahedral rotation reduces the symmetry of the T sheets to $P(3)1m$. The two T sheets within a layer are staggered by $|a|/3$ in (001) projection; therefore, in both models the ideal layer symmetry of the M layer is $C12/m(1)$ (homo- and some meso-octahedral micas) or $C12(1)$ (the remaining meso-octhaedral and all hetero-octahedral micas) (Dornberger-Schiff et al., 1982). However, the symmetry of a layer may depend on its stacking in a polytypic structure; the deviation from the ideal symmetry has been called 'desymmetrization' (Ďurovič, 1979). Desymmetrization is commonly observed in $2M_1$ and $3T$ polytypes, where the layer symmetry is usually $C\bar{1}$ and $C12(1)$, respectively (Pavese et al., 1997, 1998). In margarite-$2M_1$, further desymmetrization to $C1$ has been reported (Guggenheim & Bailey, 1975, 1978). The space-group type can allow but does not force the desymmetrization; as a matter of fact, the highest layer symmetry $C12/m(1)$ was observed, within the limit of the accuracy of the structure refinement, in coexisting $1M$ and $2M_1$ meso-octahedral oxybiotites having truly polytypic character (Ohta et al., 1982).

The origin of the M layer is usually taken in the interlayer region; the location of the origin of the O sheet in itself depends on the kind and distribution of the cations. It is always taken in the $M1$ site for homo-octahedral micas; however, in meso-octahedral micas it is in the site with different occupation and in hetero-octahedral micas corresponds to the site containing the lowest electronic density (Ďurovič et al., 1984). For these micas, the origin of the O sheet can thus be either in the $M1$ site or in one of the two $M2$ sites. As a consequence,
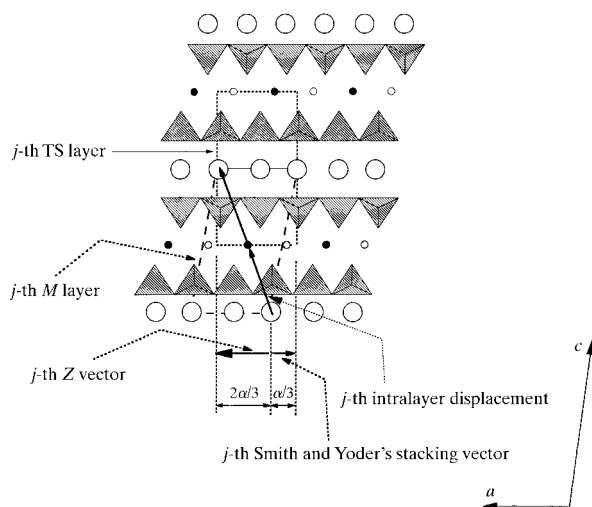

Fig. 2. Comparison between different unit layers for mica polytypes in projection along the b axis. Different kinds of stacking vectors are shown. The scale along $\mathbf{c}$ is compressed. Black and open small circles represent $M1$ and $M2$ sites, respectively. Large open circles are interlayer cations.

---

† The orthohexagonal cell used since long ago in describing micas corresponds to C_1 (e.g. Donnay et al., 1964). Other authors, such as the OD school, adopted the C_2 cell (e.g. Ďurovič et al., 1984). This different choice of the orthohexagonal cell has to be taken into account when comparing the descriptions by different authors.

two kinds of M layer exist, which are hereinafter indicated as M1 and M2, respectively, when a distinction is necessary. Their highest layer symmetries are $C12/m(1)$ and $C1(2)1$, respectively (Zvyagin, 1974). These two layers can be distinguished only if their cation distribution is known. For example, hetero-trioctahedral $1M$ micas have been refined by Backhaus (1983) (lepidolite) and Guggenheim & Bailey (1977) (zinnwaldite) in the space group $C2$. Both structures had the highest hetero-octahedral layer symmetry $C12(1)$, but the lepidolite was constructed by M1 layers whereas the zinnwaldite was built by M2 layers. Guggenheim (1981) refined a meso-octahedral lepidolite-$1M$ in the space group $C2$ with layer symmetry $C12(1)$: the cation distribution shows that the lower layer symmetry arises from the presence of the M2 layer and not from a desymmetrization of the M1 layer. The M1 layer is far more common. However, several examples of micas built by the M2 layer are known [Zvyagin *et al.*, 1985; see references in: Ďurovič *et al.*, 1984; Nespolo, 1998].

Although a single type of unit layer is sufficient to describe polytypism of micas, the choice of more than one type is suitable for some purposes. To show the OD (OD = order–disorder) character of mica polytypes, two kinds of OD layers and one kind of OD 'packet' (corresponding to half M layers) are used (Dornberger-Schiff *et al.*, 1982). To compute PID, Sadanaga & Takeda (1969) and Takeda & Sadanaga (1969) introduced four unit layers with idealized trigonal symmetry (TS unit layers), defined by two adjacent half M1 layers and the interlayer cations between them (Fig. 2). These layers are labelled D, D* [$P(\bar{3})1m$ symmetry for homo-octahedral micas], T and T* [$P(\bar{6})2m$ symmetry for homo-octahedral micas] and are staggered by means of $|a|/3$ translations along one of the equivalent hexagonal axes. D is related to D* and T to T* by a 180° rotation around c^* (Fig. 3).

1.2. Mica polytypes as OD structures: family reflections

Polytypes in which M layers are rotated by $2n \times 60°$ only are OD polytypes belonging to subfamily A (Backhaus & Ďurovič, 1984)† and the coordination polyhedron for the interlayer cations is a trigonal antiprism. Subfamily A includes the three most common homogeneous (MDO) polytypes ($1M$, $2M_1$, $3T$) and most of the inhomogeneous polytypes reported to date. On the other hand, polytypes in which M layers are rotated by $(2n + 1) \times 60°$ only are OD polytypes belonging to subfamily B (Backhaus & Ďurovič, 1984) and the coordination polyhedron for the interlayer cations is a trigonal prism. Only two homogeneous (MDO) polytypes belonging to subfamily B have been reported to date: $2M_2$ (*e.g.* Takeda & Burnham, 1969;

Černý *et al.*, 1970; Takeda *et al.*, 1971; Zhukhlistov *et al.*, 1973) and $2O$ (Giuseppetti & Tadini, 1972; Filut *et al.*, 1985). The remaining polytypes are called mixed-rotation polytypes (Nespolo, 1999); within the trigonal model, they contain both kinds of interlayer coordination polyhedra, violating the vicinity condition (Dornberger-Schiff, 1964), and thus are non-OD polytypes. They have been only seldom reported (Takeda, 1967; Bailey & Christie, 1978; Rule *et al.*, 1987; Kogure & Nespolo, 1999*a,b*) and the relatively low quality of the structure refinement does not give information on the tetrahedral rotation angle. Backhaus & Ďurovič (1984) suggested that this could be zero, thus corresponding to the Pauling model. In such a case, mixed-rotation polytypes would be OD polytypes too.

A Fourier series calculated with a three-dimensional subset of diffractions corresponding to a subgroup of translations in the reciprocal lattice gives a fictitious average structure, which is called a superposition structure. An n-fold superposition structure is obtained from a translation subgroup of order n (Dornberger-Schiff, 1964; Ďurovič, 1994*b*). Among the possible superposition structures, the one in which all the possible positions of all OD layers are simultaneously realized is of particular importance; it has also been called 'family structure' (Ďurovič, 1994*b*). The subset of the diffractions corresponding to the family structure are called family reflections; they are always sharp and are common to all the OD polytypes built on the same structural principle (Ďurovič & Weiss, 1986). The remaining ones are called non-family reflections and are typical of each polytype; they are sharp or diffuse depending on whether the polytype is ordered or not (Ďurovič, 1992, 1997; Ďurovič & Weiss, 1986; Fichtner-Schmittler, 1979; Merlino, 1997). The family reflections indicate whether a polytype belongs to subfamily A or B or it is a mixed-rotation polytype. Then, non-family reflections belonging to the (0kl) plane (common to all polytypes with the same bc projection: C_1 setting) are in principle enough to identify any polytype of mica, except homometric structures (Weiss & Wiewióra, 1986; Ďurovič, 1992).

Within the Pauling model, the family reflections are those with $h = 0 \, (\mathrm{mod} \, 3)$ and $k = 0 \, (\mathrm{mod} \, 3)$ (C_1 setting) and the family structure is ninefold (Weiss & Wiewióra, 1986). These are the only family reflections for mixed-rotation polytypes, but they are not useful for identification purposes because they are common to all polytypes of the same mineral group (Ďurovič, 1994*b*). On the other hand, within the trigonal model, the family reflections are those with $k = 0 \, (\mathrm{mod} \, 3)$ and the family structure is threefold (Weiss & Wiewióra, 1986). Family reflections corresponding to $h \neq 0 \, (\mathrm{mod} \, 3)$ show only one reflection out of N (N is the number of layers of the polytype) in the case of subfamily A, but two equally spaced reflections in the case of subfamily B (Nespolo, 1999).

---

† Takeda & Ross (1995) called ternary polytypes the OD subfamily A polytypes.
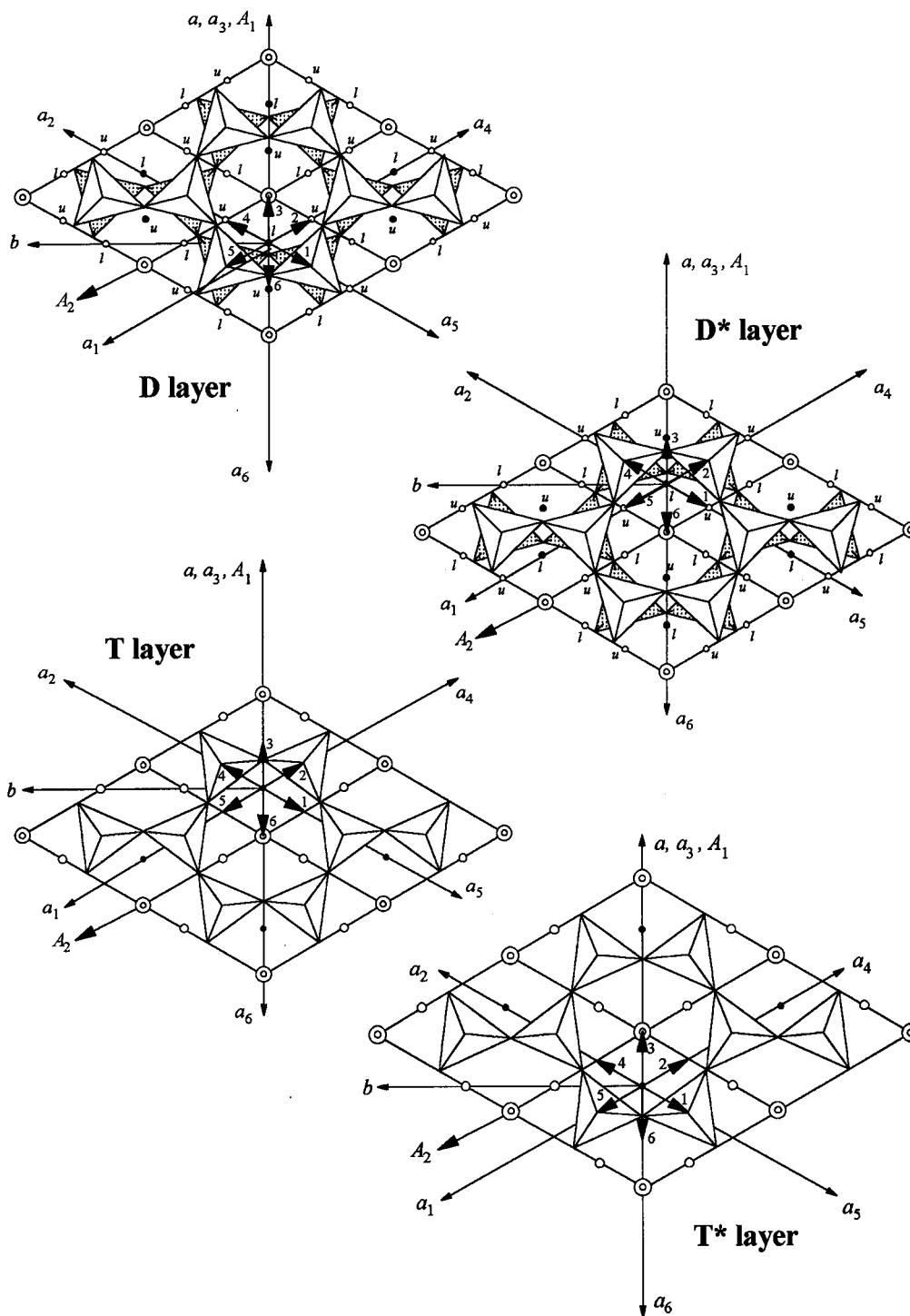
Fig. 3. The four TS unit layers. a, b: orthohexagonal axes of the C_1 setting; a_1–a_6: structure-related a orthohexagonal axes in the six possible orientations (Zhukhlistov *et al.*, 1990); A_1, A_2: hexagonal axes. The six digits 1–6 indicate the intralayer displacement vectors: these are superimposed on the projection of each of the four TS unit layers. Since each TS layer is defined from the O sheet of an M layer to the O sheet of the successive M layer, two sets of a_1–a_6 axes should be considered, both with the origin in the $M1$ site. These two sets define the orientation of the upper intralayer displacement vector of the lower M layer and of the lower intralayer displacement vector of the upper M layer. In order to improve the readability of the figure, only the first sets are shown. Black and open small circles represent $M1$ and $M2$ sites, respectively. Concentric circles represent overlapped interlayer cations and OH/F. u and l indicate octahedral cations with $z = +1/2$ and $z = -1/2$, respectively. For T and T* layers these are overlapped in (001) projection.

1.3. Lattice features

Orthogonal mica polytypes can be hexagonal (no examples known), trigonal and orthorhombic; the lattice of triclinic polytypes is metrically (pseudo-)monoclinic. Non-orthogonal polytypes are divided into *Class a* and *Class b* depending on whether the *c* axis is inclined towards the shortest or towards the longest of the two axes in the plane of the layer (Nespolo *et al.*, 1998). This classification corresponds to different values of the (001) projection of the *c* axis, labelled c_n by Zvyagin (1997). In all mica polytypes, a pseudo-hexagonal lattice can be located, which is multiple for non-orthogonal polytypes; for *Class b* polytypes this lattice is centred and a markedly pseudo-rhombohedral primitive cell exists (Nespolo, 1999). The number N of layers building a polytype can be expressed as

$$N = 3^n(3K + L), \qquad (1)$$

where K and n are non-negative integers and $L = 1$ or 2. n defines the series and L the subclass; K is a constant entering in the transformation matrices relating axial settings (Nespolo *et al.*, 1998).

1.4. Identification of the stacking sequence

The Fourier transform of a polytype is given by the Fourier transform of the stacking sequence, which is a fringe function (Lipson & Taylor, 1958), modulated by the Fourier transform of the layer(s) (Takeda, 1967). The layer transform is a nondiscrete function in the direction without periodicity, *i.e.* that indicated in parentheses in the layer symbol. When the building layers are related by just an integral submultiple of the translation period, it is possible to extract their Fourier transform from the expression of the structure factor, which thus assumes the simple form of a product of the layer transform and of the stacking sequence transform (see below). This second term expresses the periodicity in reciprocal space appearing when a structure is built by translation of subunits. This was independently recognized by Takeda (1961) and, more indirectly, by Andreeva (1962). The periodicity in reciprocal space has been used to solve the structure of zinkenite (PbS·Sb$_2$S$_3$) (Takeda, 1961; Sadanaga & Takeda, 1964; Takeda & Horiuchi, 1971) and to identify minerals with a mixed-layer structure (D'yakonov, 1962, 1963). It has been successfully applied to identify the stacking sequences of polytypes of micas (Takeda & Donnay, 1965; Ross *et al.*, 1966; Takeda, 1967), of SiC (Tokonami & Hosoya, 1965; Tokonami, 1966) and of SiC and ZnS (Farkas-Jahnke, 1966; Dornberger-Schiff & Farkas-Jahnke, 1970; Farkas-Jahnke & Dornberger-Schiff, 1970). The Fourier transform of SiC and of the ZnS unit is much different from the atomic scattering factors, and the periodicity is recognized without difficulty. In the case of micas, the unit layer is 10 Å thick and the periodicity is not easily recognized. With the obvious exception of the 1*M* polytype, subsequent layers are related by both translations and rotations. However, for a subspace of the reciprocal space, the Fourier transform of the M layer in the six possible orientations is almost unmodified (Takeda, 1967). Removal of the modulating effect of the layer gives the approximated Fourier transform of the stacking sequence. This is known as the periodic intensity distribution (PID) function (Takeda, 1967; Sadanaga & Takeda, 1969; Takeda & Sadanaga, 1969; Takeda & Ross, 1995). Comparison of calculated and observed PID values along non-family reciprocal-lattice rows parallel to c^* is in principle sufficient to identify any mica polytype (Takeda & Ross, 1995).

2. Symbolic description and layer orientation

General symbols to describe mica polytypes have been developed by the OD school (Dornberger-Schiff *et al.*, 1982; Backhaus & Ďurovič, 1984; Ďurovič *et al.*, 1984; Weiss & Wiewióra, 1986). However, for the purposes of the present research, three kinds of symbols are used here.

(i) Z symbols (Zvyagin *et al.*, 1979; Zvyagin, 1985; Zhukhlistov *et al.*, 1990) are oriented symbols giving the absolute orientation and relative displacement of half M layers. A space-fixed orthohexagonal reference is used, based on (*a*, *b*) axes [C_1 setting of Nespolo *et al.* (1998)]. The stacking sequence is indicated by the (001) projection of the *intralayer* displacement vectors, with length $|a|/3$; these vectors connect the origin of the O sheet with the nearest interlayer site and *vice versa* (the sequence of layers must be seen from the same direction). The six possible orientations of these vectors are indicated by six structure-related a_i axes ($i = 1$–6). Their (001) projection is indicated by the Z symbol i ($i = 1, 2, \ldots, 6$) when the a_i axis is parallel to the space-fixed axis *a* (Figs. 2 and 3). The complete Z symbol is $ij0kl0mn \ldots$, where 0 indicates the only *interlayer* displacement vector in micas, whose (001) components are (0, 0) (because of the presence of interlayer cations, there is no relative displacement between two neighbouring M layers in micas). Symbols giving the orientation of the two halves of an M layer (*i* and *j*, *k* and *l*, *m* and *n etc.*) must have the same parity in order to obtain an octahedral coordination for the cations. Besides, for micas built by M1 layers, $i = j$, $k = l$, $m = n$ *etc.*; the symbol 0 can be omitted and a shortened symbol $IKM \ldots$ is adopted (Zhukhlistov *et al.*, 1990; see Fig. 1 therein). For micas built by M1 layers only, the complete displacement vectors (Z vectors, hereinafter) are thus simply obtained by taking twice the intralayer displacement vectors.

(ii) RTW symbols (Ross *et al.*, 1966) are orientation-free rotational symbols giving the relative rotation between neighbouring M layers; they can be thought of as differences between pairs of shortened Z symbols. RTW symbols are written as a sequence of N digits

Table 1. *Z symbols and (a, b) components (expressed as multiples of 1/3) of the corresponding Z vectors with respect to the space-fixed reference (Zvyagin, 1967)*

Z symbol	(a, b) components	Z symbol	(a, b) components
3	$(\bar{1}, 0)$	6	$(1, 0)$
4	$(1, 1)$	1	$(1, \bar{1})$
5	$(\bar{1}, 1)$	2	$(1, \bar{1})$

$A_j = 0, \pm 1, \pm 2, 3$, the jth symbol giving the rotation angle between the jth and $(j + 1)$th M layers as an integer multiple of $60°$.†

(iii) TS symbols (Sadanaga & Takeda, 1969; Takeda & Sadanaga, 1969) give the relative positions of TS unit layers by means of only displacements and no rotations. TS symbols are written as a sequence of N symbols $L_j(\Delta X_j, \Delta Y_j)$, $1 \leq j \leq N$, where L_j is the kind of layer, (D, D*, T, T*) and $(\Delta X_j, \Delta Y_j)$ are the (A_1, A_2) components of the shift vector between the jth TS layer and the Nth TS layer of the previous repeat (Fig. 2).

Only Z symbols can distinguish between M1 and M2 layers. Since PID is computed by means of TS symbols (see below), the stacking sequence obtained from PID analysis is the one for homo-octahedral micas. Therefore, hereinafter the approximation M1 = M2 = M is called the homo-octahedral approximation.

The stacking sequence of mica polytypes is quite often described by means of the stacking vectors according to the original definition of Smith & Yoder (1956), *i.e.* the (001) projection of vectors connecting two nearest interlayer cations on the two sides of a layer (Fig. 2). Unlike Z vectors, these vectors do not pass through any cation site in the O sheet. Therefore, stacking vectors of Smith & Yoder (1956) cannot distinguish between M1 and M2 layers and they too correspond to the homo-octahedral approximation.‡

Both the M layer and the TS unit layers have the origin in the interlayer region. However, TS unit layers are shifted along [001] by half the thickness of the M layer (Fig. 2) (Sadanaga & Takeda, 1969; Takeda & Sadanaga, 1969); therefore, the origin of the jth TS unit layer is in the interlayer region where the origin of the $(j + 1)$th M layer is located. Besides, the jth TS unit layer is defined by the relation between the jth and the $(j + 1)$th M layers: D and D* layers appear in the middle of two M layers rotated by $2n \times 60°$ [*i.e.* the RTW symbol is $A_j = 0 \,(\mathrm{mod}\, 2)$], while T and T* layers appear

in the middle of two M layers rotated $(2n + 1) \times 60°$ [*i.e.* $A_j = 1 \,(\mathrm{mod}\, 2)$].

The origin of Zvyagin's coordinate vectors is in the O sheet, but Z vectors are defined as the (001) projection of the vectors passing through the origin of the O-sheet site and connecting two interlayer sites below and above an M layer (Zvyagin *et al.*, 1979). The jth Z vector gives thus the (a, b) components of the displacement between the jth and the $(j + 1)$th M layers (Fig. 2). As seen above, in the homo-octahedral approximation, Z vectors are just twice the intralayer displacement vectors; their (a, b) components are given in Table 1.

The four TS unit layers, together with intralayer displacement vectors, are shown in Fig. 3. In these layers, the atoms have identical coordinates except those of M_O and O_B, the hexagonal coordinates of which are presented in Table 2 (Sadanaga & Takeda, 1969; Takeda & Sadanaga, 1969). The lower octahedral sheet of the jth TS layer is the octahedral sheet of the jth M layer. By labelling o (odd) and e (even) the orientation parity of Z symbols of half layers, the following correspondences with the complete Z symbols are obtained from Fig. 3:

$$D = o0o; \quad D^* = e0e; \quad T = e0o; \quad T^* = o0e. \quad (2)$$

3. PID in terms of TS unit layers

Every mica polytype can be approximately described by means of one or more TS unit layers, with mutual staggers of $|a|/3$ along one of the hexagonal axes (Sadanaga & Takeda, 1969; Takeda & Sadanaga, 1969), and two neighbouring TS layers must connect a half M layer with the same orientation parity. On the basis of equations (2), there are only eight possible pairs of TS unit layers (DD; D*D*; TT*; T*T; DT*; D*T; TD; T*D*). Besides, in order to match the cation positions, the layer stacked over a D or T layer has to be shifted by $-a/3$, whereas the layer stacked over a D* or T* layer has to be shifted by $+a/3$ (Table 2). The Fourier transform of an N-layer mica polytype in terms of TS unit layers in hexagonal axes is expressed as [modified after Takeda & Sadanaga (1969)]:

$$G^N(HK.L) = \sum_{j=1}^{N} G_j(HK.L_R) \exp \left\{ 2\pi i [H\Delta X_j + K\Delta Y_j \right.$$
$$\left. + L(j - 1)/N] \right\}. \quad (3)$$

$G_j(HK.L_R)$ is the Fourier transform of the jth TS unit layer, which is two-dimensionally periodic. In the direction without periodicity, the reciprocal-lattice coordinate is not restricted to integral values but is a real variable and is here labelled L_R. In equation (3), G_j plays a role analogous to that of the atomic scattering factor in the expression of the structure factor.

As shown above, the atomic coordinates in the four TS unit layers differ only for O_B and M_O, but within the

---

† It is now common to see RTW symbols written inside square brackets; their use was not specified by the authors in their original paper (Ross *et al.*, 1966).

‡ Stacking vectors similar to those of Smith & Yoder (1956) were introduced earlier by Dekeyser & Amelinckx (1953) as the projection of the vector connecting two OH/F sites within an M layer. A numerical symbolism similar to that of Zvyagin and co-workers was also introduced, which, however, considered whole M layers and not half M layers. The description by Dekeyser & Amelinckx (1953) is correct in the homo-octahedral approximation.

Table 2. *Hexagonal coordinates of the octahedral cations and basal oxygen atoms in the upper and lower halves of the four TS unit layers*

The coordinates of symmetry-independent atoms only are given. The hexagonal axes within the layer are assumed to have A_1 coincident with a of the space-fixed reference (see Fig. 3). $f(\alpha)$ and $f(\psi)$ are functions of the ditrigonal rotation (α) and of the octahedral flattening (ψ) and are given in Table 1 of Takeda & Ross (1995).

	D	D*	T	T*
Upper M_O	$(1/3, 0, 1/2)$	$(\bar{1}/3, 0, 1/2)$	$(1/3, 0, 1/2)$	$(\bar{1}/3, 0, 1/2)$
Lower M_O	$(\bar{1}/3, 0, \bar{1}/2)$	$(1/3, 0, \bar{1}/2)$	$(1/3, 0, \bar{1}/2)$	$(\bar{1}/3, 0, \bar{1}/2)$
Upper O_B	$[1/2 - f(\alpha), 0, 1/2 + f(\psi)]$	$[1/2 + f(\alpha), 0, 1/2 + f(\psi)]$	$[1/2 + f(\alpha), 0, 1/2 + f(\psi)]$	$[1/2 - f(\alpha), 0, 1/2 + f(\psi)]$
Lower O_B	$[1/2 + f(\alpha), 0, 1/2 - f(\psi)]$	$[1/2 - f(\alpha), 0, 1/2 - f(\psi)]$	$[1/2 + f(\alpha), 0, 1/2 - f(\psi)]$	$[1/2 - f(\alpha), 0, 1/2 - f(\psi)]$

Table 3. *Relation between the integral hexagonal L_N index referred to an N-layer cell and the real L_R orthogonal reciprocal-lattice coordinate of the Fourier transform of the layer*

	Orthohexagonal (a, b) axes	Hexagonal (A_1, A_2) axes
Orthogonal polytypes	$L_R = L_N/N$	$L_R = L_N/N$
Class a polytypes	$L_R = L_N/N + h/3N$	$L_R = L_N/N + H/3N$
Class b polytypes	$L_R = L_N/N + k/3N$	$L_R = L_N/N + (H + 2K)/3N$

Pauling model the O_B atoms also take the same ideal coordinates in all the four TS unit layers (Table 2). Besides, the contributions from the M_O cations to the layer Fourier transform become identical when the following conditions are satisfied (*cf.* Sadanaga & Takeda, 1969; Takeda & Sadanaga, 1969; Takeda & Ross, 1995):

$$H = 0\,(\text{mod}\,3), \quad \text{all } K;$$
$$H = 1\,(\text{mod}\,3), \quad K \neq 1\,(\text{mod}\,3);$$
$$H = 2\,(\text{mod}\,3), \quad K \neq 2\,(\text{mod}\,3);$$
$$h = 0\,(\text{mod}\,3), \quad \text{all } k;$$
$$h \neq 0\,(\text{mod}\,3), \quad k \neq 0\,(\text{mod}\,3). \tag{4}$$

Consequently, G_j is identical for all j ($G_j = G_0$) and the contribution of the Fourier transform of the layer can be extracted from the summation in (3), obtaining the PID function S^N:

$$S^N(HK.L) \cong G^N(HK.L)/G_0(HK.L_R)$$
$$= \sum_{j=1}^{N} \exp\left\{2\pi i[H\Delta X_j + K\Delta Y_j + L(j-1)/N]\right\}. \tag{5}$$

Since the non-90° angle can be either α or β, the relation between L and L_R depends on the *Class* and is given in Table 3 for orthohexagonal (h, k) and hexagonal (H, K) indices.

PID as defined in equation (5) exists in a subspace of the reciprocal space, which is identified by equation (4). As shown by Sadanaga & Takeda (1969) (see their Fig. 4), (4) locates the subspace of the non-family reflections plus reciprocal-lattice rows parallel to $\mathbf{c}^*$ with both h and $k = 0\,(\text{mod}\,3)$; these reflections, as stated above, are

family reflections corresponding to the ninefold family structure (common to all mica polytypes).

Within the trigonal model, the O_B atomic coordinates are no longer identical; however, from Table 2 and Fig. 3 it is easy to verify that the O_B contribution to G_j in all the four TS unit layers is the same when

$$H = 0, \quad \text{all } K; \quad K = 0, \quad \text{all } H; \quad H = -K;$$
$$h = 0, \quad \text{all } k; \quad h = \pm k. \tag{6}$$

For these reflections, $G_j = G_0$ and equation (5) holds again.

Finally, PID is defined in a subspace of the reciprocal space, which narrows from polytypes of subfamily A to mixed-rotation polytypes in the following way (Fig. 4).

(i) Polytypes of subfamily A involve only $2n \times 60°$ rotations of the M layer (same orientation parity of Z symbols; all-even RTW symbols) and are thus described by only one kind of TS layer (D or D* depending on the orientation parity; see next paragraph). Therefore, equation (5) is valid in the whole reciprocal space. For identification of individual polytypes, PID calculated along each of the reciprocal-lattice rows parallel to $\mathbf{c}^*$ and belonging to non-family reflections can be used.

(ii) Polytypes of subfamily B involve only $(2n + 1) \times 60°$ rotations of the M layer (alternating orientation parity of Z symbols; all-odd RTW symbols). For these polytypes, both T and T* layers are necessary; in fact [equation (2)] TT* and TT* pairs are physically possible, whereas TT and T*T* pairs are not. In these two TS layers, the x coordinates of O_B atoms are identical (Table 2). Therefore, equation (5) is valid under the conditions given by (4). For identification purposes, PID in the whole subspace of the non-family reflections can be used also in this case.

(iii) Mixed-rotation polytypes correspond to different non-alternating orientation parity of Z symbols, *i.e.* both even and odd RTW symbols; in general, they require all the four TS unit layers and equation (5) is valid only under the conditions given by (6). Therefore, PID is defined only for reciprocal-lattice rows parallel to $\mathbf{c}^*$ and belonging to the three planes $(0kl)$, (hhl), $(\bar{h}hl)$, which correspond to the first, third, fifth, eight, eleventh, ... ellipses of the oblique-texture electron diffraction technique (Zvyagin, 1967).

In conclusion, PID is always defined at least in the three planes $(0kl)$, (hhl) and $(\bar{h}hl)$.

4. TS layers and choice of the axial setting

The theory of axial settings recently introduced (Nespolo *et al.*, 1998) aims at a unified geometrical treatment of the lattice of mica polytypes, mainly in view of dealing with the long-period polytypes, the stacking sequence of which can be determined by PID analysis. A crucial step in order to compute PID is the determination of the space orientation of the structural model in accordance with its space-group type. The correct procedure is analysed hereinafter in terms of *Series*, *Classes* and *Subclasses*, which represent the basis for the choice of the most suitable structure-related axial setting.
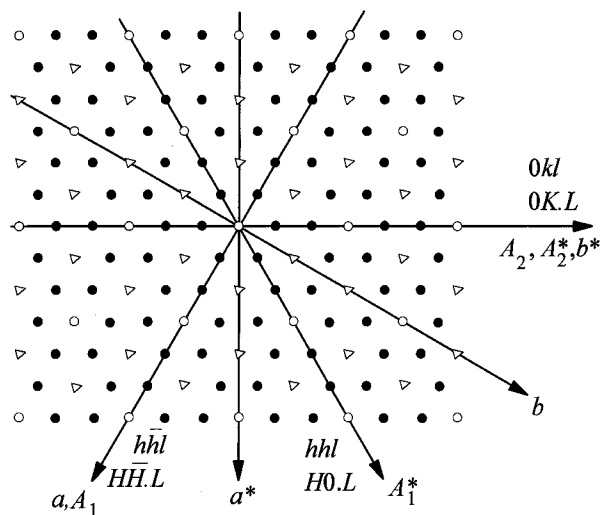

Fig. 4. (001) projection of mica reciprocal lattice. Direct- and reciprocal-lattice axes are shown, not on the same scale (hexagonal axes: A_1, A_2, A_1^*, A_2^*; orthohexagonal axes: a, b, a^*, b^*). The orthohexagonal axes locate the C_1 cell [*cf.* Fig. 2 of Nespolo, Takeda & Ferraris (1997)]. Open circles: family reflections for the ninefold family structure (common to all mica polytypes). Open triangles: family reflections for the threefold family structure but not for the ninefold one (different for subfamily A and subfamily B OD polytypes). Black circles: non-family reflections. The three planes indicated (*hkl*: orthohexagonal indices; *HK.L*: hexagonal indices) are the only ones in which PID is defined in the case of mixed-rotation polytypes [modified after Sadanaga & Takeda (1969)].

In *Series* 0 [$n = 0$ in equation (1)], polytypes of subfamily A belong to *Class a*. By imposing $\mathbf{c}_n = (\bar{1}/3, 0)$, it is easy to show that *Subclass* 1 polytypes are described by all-odd Z symbols (D layers only), whereas *Subclass* 2 polytypes are described by all-even Z symbols (D* layers only). The origin of each layer is displaced by $-1/3$ (D layers) or $+1/3$ (D* layers) along the a axis and 0, $\pm 1/3$ along the b axis of the C_1 setting. The c axis passes through the origin of each layer and in *Subclass* 1 it is displaced by $-a/3$ for *each* stacking of layers; the resulting monoclinic angle is β_{1M}. On the other hand, in *Subclass* 2, the c axis is displaced $+a/3$ for *each* stacking of layers and the resulting monoclinic angle is $\pi - \beta_{1M}$, *i.e.* an acute monoclinic angle. For *Subclass* 2 polytypes, it is convenient to choose a monoclinic axial setting having $\mathbf{c}_n = (1/3, 0)$, so that only the D layer is needed and the c axis is again shifted by $-1/3$ along $\mathbf{a}$ for each stacking of layers, with a resulting monoclinic angle β_{1M}. The correspondence between Z symbols and D/D* layers is, however, inverted, since Z symbols are defined with respect the C_1 setting and thus do not change. Taking the translationally reduced total displacement along the $-a$ semi-axis for *Subclass* 1 polytypes and along the $+a$ semi-axis for *Subclass* 2 polytypes, all *Series* 0 subfamily A polytypes can be described by only D layers, with (ideally) the same obtuse monoclinic angle of the $1M$ polytype. The axial setting for *Series* 0 subfamily A polytypes corresponds thus to the Fixed-angle setting ($^a\mathbf{F}$), introduced by Nespolo *et al.* (1998); for all polytypes belonging to a given *Series*, this setting has (ideally) the same monoclinic angle of the first (*i.e.* shortest period) polytype of that *Series*. Therefore, for *Series* 0 subfamily A polytypes, the simplest layer description (by means of D layers only) corresponds to the choice of the $^a\mathbf{F}$ axial setting.

In the case of a higher *Series*, polytypes of subfamily A are either orthogonal or belong to *Class b*; in the second case, the simple relation between the *Subclass* and the parity of Z symbols (and thus the kind of TS layer), seen in the case of *Series* 0, is no longer valid. In fact, in *Class b* the parity of Z symbols depends on the relative proportion of 0, 2 and -2 digits in the RTW symbols, and on their sequence. Besides, for subfamily B and for mixed-rotation polytypes, two and more than two different TS unit layers are necessary, respectively, and the displacement of each layer is not always in the same direction. The choice of the Fixed-angle axial settings $^{(3^n,a;3^n,b)}\mathbf{F}$ (Nespolo *et al.*, 1998) generalizes the criterion valid for *Series* 0 subfamily A polytypes and is the most natural setting when calculating PID by means of TS layers. Furthermore, for an N-layer polytype, the PID function $S^N(l_N)$ is periodic with $l_N = 0, N - 1$, where l_N is the diffraction index referred to the N-layer unit cell. Since the origin of $S^N(l_N)$ is not fixed *a priori*, when comparing the computed and observed PID values, in principle the cyclic permutations of the N

Table 4. *Transformation rules for Z symbol sequences under the effect of the symmetry operators of the hexagonal syngony*

IJ . . . P is the original sequence of Z symbols. Proper and improper motions have representation matrices with determinants $+1$ and -1, respectively. Indexing is in orthohexagonal axes.

Proper motion	Effect on Z-symbol sequence	Improper motion	Effect on Z-symbol sequence
$[001]_{2n\pi/6}$	$n+I, n+J, \ldots, +n+P$	(001)	$3+P, \ldots, 3+J, 3+I$
$[100]_\pi$	$3-P, \ldots, 3-J, 3-I$	(100)	$3-I, 3-J, \ldots, 3-P$
$[310]_\pi$	$4-P, \ldots, 4-J, 4-I$	(110)	$4-I, 4-J, \ldots, 4-P$
$[110]_\pi$	$5-P, \ldots, 5-J, 5-I$	(130)	$5-I, 5-J, \ldots, 5-P$
$[3\bar{1}0]_\pi$	$8-P, \ldots, 8-J, 8-I$	$(1\bar{1}0)$	$8-I, 8-J, \ldots, 8-P$
$[1\bar{1}0]_\pi$	$7-P, \ldots, 7-J, 7-I$	$(1\bar{3}0)$	$7-I, 7-J, \ldots, 7-P$
$[010]_\pi$	$6-P, \ldots, 6-J, 6-I$	(010)	$6-I, 6-J, \ldots, 6-P$
		$\hat{i}$	$P, \ldots, JI$

values should be tried, as well as the inverse sequence. In the $^{(3^n,a;3^n,b)}F$ axial setting, the origin is automatically fixed and that necessity is thus removed. However, special attention is needed in the case of triclinic polytypes belonging to *Class b* and *Series* higher than 0 (see §8).

5. Structural model orientation and symbol conversion

The six possible orientations of the structural model of each polytype with respect to the (a, b) axes correspond to one and the same RTW symbol, but to six different sequences of both Z symbols and TS symbols, and are in general non-equivalent. Taking into account that:

(*a*) c_n, translationally reduced, assumes components $(0, 0)$ (orthogonal polytypes), $(\pm 1/3, [0, \pm 1/3])$ (*Class a* polytypes) and $(0, \pm 1/3)$ (*Class b* polytypes);

(*b*) by rotation around c^*, c_n for *Class a* polytypes can always be reduced to $(\pm 1/3, 0)$ (Zvyagin, 1962, 1997); the six orientations of the structural model can be grouped in the following way.

(*a*) *Class a polytypes*. Each orientation corresponds to a different c_n projection.

(*b*) *Class b polytypes*. Three orientations correspond to $c_n = (0, 1/3)$ and three others to $c_n = (0, \bar{1}/3)$. The three orientations with the same c_n components are equivalent in the case of triclinic polytypes, but not for monoclinic ones. The symmetry elements in the C_1 setting must be disposed according to an *a*-unique setting. Only one of the three orientations leading to $c_n = (0, \bar{1}/3)$ agrees with such a requirement.

(*c*) *Orthogonal polytypes*. All the six orientations correspond to $c_n = (0, 0)$ and they are equivalent for hexagonal, trigonal and triclinic polytypes, while for orthorhombic and monoclinic polytypes only two orientations, related by a 180° rotation around the $c = c^*$ axis, lead to the correct disposition of the symmetry elements.

The PID computation procedure described by Takeda & Ross (1995) takes into account only the numerical values of c_n and not the equivalence/non-equivalence relations. It is thus incomplete for *Class b* and orthogonal polytypes. By redefining the stacking operators r_j

introduced by Takeda & Ross (1995) in terms of Z symbols, the correct structural model orientation can be obtained by analysing the symmetry properties of these symbols. Then, the calculation of the PID function requires the following steps.

Step 1 is the conversion from RTW symbols to 'provisional' Z symbols, by simply looking for $c_n = (0, 0)$, $(\bar{1}/3, 0)$ or $(0, \bar{1}/3)$. This is straightforwardly obtained by means of a simple addition cycle:

$$Z_j = Z_{j-1} + A_{j-1} \quad (j = 2 - N). \tag{7}$$

$Z_1 = 3$ is assumed at first; if the resulting c_n projection does not take one of the three expected values, Z_1 is incremented and equation (7) is recalculated.

Step 2 is the derivation of the correct Z symbols, by analysing their symmetry properties. Symbols calculated by means of equation (7) display the full symmetry of the polytype. However, for orthogonal and *Class b* polytypes, they may correspond to an orientation of the symmetry elements not compatible with the space-group type. In such a case, the sequence of Z symbols must be changed, by making Z_1 take one of the other values leading to the same c_n. This is tantamount to rotating the structural model around c^*. The space-group type needs to be checked among only the 24 possible ones (Takeda, 1971) [for the relation between the two-dimensional pseudo-hexagonal and hexagonal lattices in the plane of the layer, see Nespolo, Takeda & Ferraris (1997) and Nespolo, Takeda, Ferraris & Kogure (1997)]. The symmetry properties of Z symbols for micas can be numerically expressed as in Table 4, where the original sequence of Z symbols is assumed to be IJ . . . P. The correct sequence is found when Z symbols are related by symmetry operators located along the lattice directions compatible with the requirements of the space-group type.

Step 3 is the expression of the stacking operators r_j (Takeda & Ross, 1995) as a function of Z symbols and calculation of TS symbols. The stacking operators r_j are here redefined as giving the displacement between the $(j-1)$th and the jth TS layers. Their (a, b) components are indicated as (x_{r_j}, y_{r_j}). The relation of the stacking operators r_j with Z symbols is straightforward

Table 5. *Expression of the kind of TS unit layer L_j in terms of RTW symbols A_j and stacking operators r_j*

	r_j	
A_j	0 (mod 2)	1 (mod 2)
0 (mod 2)	$L_j = D^*$	$L_j = D$
1 (mod 2)	$L_j = T^*$	$L_j = T$

for orthogonal polytypes, while for non-orthogonal polytypes the *Subclass* has to be taken into account. Z symbols for non-orthogonal polytypes always correspond to $(\bar{1}/3, 0)$ (*Class a*) or $(0, \bar{1}/3)$ (*Class b*). PID is most conveniently expressed in the $^{(3^n, a; 3^n, b)}\mathbf{F}$ axial setting, which corresponds to $\mathbf{c}_n = (\bar{1}/3, 0)$ or $(0, \bar{1}/3)$ for *Subclass* 1 and $\mathbf{c}_n = (1/3, 0)$ or $(0, 1/3)$ for *Subclass* 2. It follows that for orthogonal polytypes and *Subclass* 1 polytypes the stacking operators simply coincide with Z symbols ($r_j = Z_j$), while for *Subclass* 2 polytypes they are related by a 180° rotation around $\mathbf{c}^*$ ($r_j = Z_j + 3$).

Step 4 is the computation of the PID (S^N) as a function of (a, b) components of TS symbols. The components of the jth TS layer referred to the (a, b) axes are indicated as (X_j, Y_j), to distinguish them from the components in the (A_1, A_2) axes, which were labelled $(\Delta X_j, \Delta Y_j)$ [equations (3) and (5)]. (X_j, Y_j) are just the sum of the (x_{r_j}, y_{r_j}) components from the first to jth stacking operators. However, since the c axis of the $^{(3^n, a; 3^n, b)}\mathbf{F}$ axial setting is displaced by $-1/3^{(n+1)}$ (where n is the *Series*) along a or b (depending upon the *Class*), the additional displacement $[-j/3^{(n+1)}, 0]$ (*Class a*) or $[0, -j/3^{(n+1)}]$ (*Class b*) must be added to the (X_j, Y_j) component of the jth TS symbol to express the layer stacking of non-orthogonal polytypes with respect to the $^{(3^n, a; 3^n, b)}\mathbf{F}$ axial setting. In this way, TS symbols for *Series* 0 subfamily A polytypes always have $X_j = 0$ (c axis passing through the origin of each layer).

$$
\left\{
\begin{array}{l}
\text{Orthogonal polytypes:} \\
\quad (X_j, Y_j) = \sum_{i=1}^{j} (x_{r_i}, y_{r_i}) \\
\text{\textit{Class a} polytypes:} \\
\quad (X_j, Y_j) = \sum_{i=1}^{j} (x_{r_i}, y_{r_i}) + (-i/3^{n+1}, 0) \qquad (8) \\
\text{\textit{Class b} polytypes:} \\
\quad (X_j, Y_j) = \sum_{i=1}^{j} (x_{r_i}, y_{r_i}) + (0, -i/3^{n+1}).
\end{array}
\right.
$$

Finally, in *Class b* the axes exchange $a \leftrightarrow b$ has to be accomplished in order to obtain the $^{3^n, b}\mathbf{F}$ axial setting. The complete TS symbols $L_j(X_j, Y_j)$ are easily obtained from Table 5 and (8), and the PID function S^N is given in equation (9) [after Takeda & Sadanaga (1969), notation slightly modified].

$$
\begin{aligned}
S^N(hk\hat{l}) &= \sum_{j=1}^{N} S_j^N(hk\hat{l}) \\
&= \sum_{j=1}^{N} \exp\left\{2\pi i[hX_j + kY_j + \hat{l}(j-1)/N]\right\} \\
&\qquad\qquad [\hat{l} = l \,(\mathrm{mod}\, N)] \qquad (9)
\end{aligned}
$$

with the normalizing condition

$$
\sum_{j=1}^{N} [S_j^N(hk\hat{l})]^2 = N^2. \qquad (10)
$$

It should be considered that equation (5) is based on the approximation of a trigonal distribution of each kind of atom in the layer and G_0 is thus an approximation of the Fourier transform of the layer. In the regions of the reciprocal space where G_0 passes through zero and changes sign, the relative error becomes large and equation (5) is actually no longer applicable. In the practice of mica polytype identification, the periods corresponding to l intervals including those regions should not be used to derive the PID from measured intensities. These intervals depend on the actual chemical composition.

6. Symmetry of PID

The PID function in equation (9) can be rewritten as

$$
S^N(hk\hat{l}) = \sum_{j=1}^{N} \exp(2\pi i \varphi_j) \exp\left\{2\pi i[\hat{l}(j-1)/N]\right\}, \quad (11)
$$

where

$$
\varphi_j = hX_j + kY_j.
$$

Similarly,

$$
\begin{aligned}
S^N(2h, 2k, N - \hat{l}) &= \sum_{j=1}^{N} \exp(2\pi i 2\varphi_j) \exp\Big\{2\pi i \\
&\qquad \times [(N - \hat{l})(j-1)/N]\Big\}. \quad (12)
\end{aligned}
$$

For *Series* 0 polytypes, φ_j can assume only the three values 0, 1/3 or 1/3; it follows that:

$$
\left\{
\begin{array}{l}
\cos(2\pi 2\varphi_j) = \cos(2\pi\varphi_j) = \cos[2\pi(-\varphi_j)] \\
\sin(2\pi 2\varphi_j) = -\sin(2\pi\varphi_j) = \sin[2\pi(-\varphi_j)].
\end{array}
\right. \qquad (13)
$$

Also,

$$
\left\{
\begin{array}{l}
\cos\{2\pi[(N - \hat{l})(j-1)/N]\} = \cos\{2\pi[\hat{l}(j-1)/N]\} \\
\sin\{2\pi[(N - \hat{l})(j-1)/N]\} = -\sin\{2\pi[\hat{l}(j-1)/N]\}
\end{array}
\right.
$$

$$
(14)
$$

and thus

$$
S^N(2h, 2k, \hat{l}) = S^N(h, k, N - \hat{l}). \qquad (15)
$$

For *Series* 0 subfamily A polytypes, φ_j in equation (11) simply becomes kY_j and, once more, it can assume only

Table 6. *Symbols, reflection conditions and PID values for subfamily A orthogonal polytype (C_1 setting; hexagonal setting within parentheses)*

Polytype	Space-group type	RTW	Z	TS	Reflection conditions	PID (02l)
3T	$P3_112$	$[2]_3$	351	D$(-1,0)$D$(1,1)$D$(0,0)$	$k = 3n$: $l = 3n + h$	1.7, 1.7, 1.7
	$P3_212$	$[2]_3$	315	D$(-1,0)$D$(1,-1)$D$(0,0)$	$[H - K = 3n$: $L = 3n + H]$	1.7, 1.7, 1.7

the three values 0, 1/3 or $-1/3$. From equations (12) and (14), it follows that

$$S^N(0, 2k, \hat{l}) = S^N(\overset{\pm}{\bar{k}}\,\bar{k}\,\hat{l}) = S^N(\overset{\pm}{\bar{k}} k, N - \hat{l}). \qquad (16)$$

For all polytypes belonging to *Series* 0, the following relations hold [see equation (14)]:

$$S^N(04\hat{l}) = S^N(02, N - \hat{l});$$
$$S^N(22\hat{l}) = S^N(11, N - \hat{l}); \qquad (17)$$
$$S^N(\bar{2}2\hat{l}) = S^N(\bar{1}1, N - \hat{l}).$$

Besides, in the case of OD polytypes, for which the PID is defined in the whole subspace of non-family reflections, since in *Series* 0, X_j and Y_j may take only 0, $\pm 1/3$, the following general relation holds:

$$S^N(h + 3N, k + 3N, \hat{l}) = S^N(hk\hat{l}). \qquad (18)$$

Polytypes of subfamily A are described by only one kind of TS layer (D or D*) and the component X_j in equations (8) and (9) is always zero. Equation (16) shows that the distribution of the PID values has a trigonal symmetry, obeying the following relation:

$$S^N(02\hat{l}) = S^N(\bar{1}\bar{1}\hat{l}) = S^N(1\bar{1}\hat{l}) = S^N(0\bar{2}, N - \hat{l})$$
$$= S^N(11, N - \hat{l}) = S^N(\bar{1}1, N - \hat{l}). \qquad (19)$$

Therefore, in Tables 6–14, only $S^N(02\hat{l})$ will be given for subfamily A *Series* 0 polytypes.

For higher *Series*, equations (17) and (18) are satisfied for orthogonal polytypes, but the length of the axis displacement for non-orthogonal polytypes is a submultiple of the layer stagger [see equation (8) and §8] and the same PID values correspond to different l indices. With respect to equation (17), an origin shift and the inversion in the reading sequence appear, which depend in a complex way on h and k. Subfamily A polytypes of *Series* > 0 never belong to *Class a*; the c axis is either perpendicular (orthogonal polytypes) or inclined towards b (*Class b*); for a 3N-layer polytype, the X_j components corresponding to $j = 0, 1, 2 \,(\mathrm{mod}\,3)$ take the sequences $(1/3, \bar{1}/3, 0)_N$ or $(1/3, 1/3, 0)_N$ depending on the orientation parity and, for *Class b* polytypes, on the *Subclass*. Again, because of the fractional relation between axis displacement and the layer stagger, an origin shift occurs and equation (18) is no longer satisfied. Finally, in the case of subfamily B and mixed-rotation polytypes, more than one kind of TS unit layer is required and X_j can take all the possible values

in different sequences, depending on the polytype. As a consequence, equation (19) reduces to the centro-symmetrical relation $S^N(hk\hat{l}) = S^N(\bar{h}\bar{k}, N - \hat{l})$.

7. Reflection conditions

In the diffraction patterns of mica polytypes, systematic absences are due either to the space-group type [general reflection conditions (Hahn & Vos, 1996)] or to local symmetry [additional reflection conditions (Hahn & Vos, 1996), Templeton effect (Templeton, 1956; Pabst, 1959, 1961; Rumanova & Belov, 1961), non-characteristic orbits of space groups (Wondratschek, 1976; Matsumoto & Wondratschek, 1979, 1987)]. These absences may affect part or all of the non-family reflections. The reflection conditions are part of the information contained in the PID function. PID is however defined only for a subspace of the non-family reflections, at least for mixed-rotation polytypes. For these polytypes, the reflection conditions appearing in the subspace where PID is not defined may convey some information useful for a preliminary analysis. The complete reflection conditions for mica polytypes can be obtained by Zvyagin's functions (Zvyagin, 1967; Nespolo & Kogure, 1998), *i.e.* by a form of the structure factor parameterized *versus* the features of the polytypes. Since the number of polytypes grows very rapidly with the number of layers, in Tables 6–14 the complete reflection conditions for mica polytypes with up to four layers only are given.

There are 1, 2, 6 and 26 possible mica polytypes with 1, 2, 3 and 4 layers, respectively, listed by Ross *et al.* (1966). Tables 6–14 give space-group type, RTW, Z and TS symbols, calculated reflection conditions and computed PID values for these polytypes in the C_1 (orthogonal polytypes) or $^{(3^n,a;3^n,b)}$F axial settings (non-orthogonal polytypes). Hexagonal indices for the 3T polytype are written in capital letters. In the real structure, the additional reflection conditions correspond to low but nonzero values of the structure factor: this is especially true in the case of dioctahedral micas, where one of the octahedral sites is more distorted and (ideally) vacant, although not always completely (Pavese *et al.*, 1997), and the corresponding weak reflections have been called 'dioctahedral reflections' (Rieder, 1968).

Table 7. *Symbols, reflection conditions and PID values for subfamily B orthogonal polytypes (C_1 setting)*

Polytype	Space-group type	RTW	Z	TS	Reflection conditions	PID 02l	11l	−11l
2O	Cccm	[3]$_2$	36	T(−1, 0)T*(0, 0)	$h = 3n$: $l = 2n$	2.0, 0.0	1.0, 1.7	1.0, 1.7
4M$_6$	C2/c	1$\bar{1}$11	3432	T(−1,0)T*(0,1)T(−1,1)T*(0,0)	$h = 3n, k = 3n$: $l = 4n$	2.0, 2.45, 0.0, 2.45	1.0, 3.3, 1.7, 0.9	1.0, 0.9, 1.7, 3.3
					$h = 3n, k \neq 3n$: $l \neq 4n + 2$			
					$h \neq 3n, k = 3n$: $l = 2n$			

Table 8. *Symbols, reflection conditions and PID values for mixed-rotation orthogonal polytypes (C_1 setting)*

Polytype	Space-group type	RTW	Z	TS	Reflection conditions	PID 02l	11l	−11l
4O$_1$	Ccmm	0303	3366	D(−1,0)T(1,0)D*(−1,0)T*(0,0)	$h = 3n$: $l = 4n$	4.0, 0.0, 0.0, 0.0	1.0, 1.7, 3.0, 1.7	1.0, 1.7, 3.0, 1.7
4O$_2$	C2cm	13$\bar{1}$3	1254	T(−1, −1)T*(0,1)T(−1, −1)T*(0,0)	$h = 3n, k = 3n$: $l = 4n$	1.0, 1.7, 3.0, 1.7	2.6, 1.7, 1.7, 1.7	2.6, 1.7, 1.7, 1.7
					$h \neq 3n, k = 3n$: $l = 2n$			
4O$_3$	Cc2m	23$\bar{2}$3	2415	D*(1, −1)T*(−1,0)D(1, −1)T(0,0)	$h = 3n, k = 3n$: $l = 4n$	2.0, 0.0, 3.5, 0.0	2.6, 1.7, 1.7, 1.7	2.6, 1.7, 1.7, 1.7
					$h = 3n, k \neq 3n$: $l = 2n$			
4O$_4$	C222$_1$	1212	1245	T(−1, −1)D*(0,1)T*(1, −1)D(0,0)	$h = 3n, k = 3n$: $l = 4n$	1.0, 1.7, 3.0, 1.7	2.0, 2.45, 0.0, 2.45	2.0, 2.45, 0.0, 2.45
					$h \neq 3n, k \neq 3n$: $l \neq 4n + 2$			
4M$_7$	C2	01$\bar{2}$1	3342	D(−1,0)T(1,0)D*(−1,1)T*(0,0)	$h = 3n, k = 3n$: $l = 4n$	2.6, 1.7, 1.7, 1.7	1.0, 3.3, 1.7, 0.9	1.0, 0.9, 1.7, 3.3

Table 9. *Symbols, reflection conditions and PID values for subfamily A Series 0 Class a polytypes (^{a}F setting)*

Polytype	Space-group type	RTW	Z	TS	Reflection conditions	PID (02l)
$2M_1$	$C2/c$	$2\bar{2}$	24	D(0,1)D(0,0)	$k = 3n: l = 2n$	1.0, 1.7
$4M_1$	$C2/c$	$020\bar{2}$	5511	D(0,1)D(0,−1)	$k = 3n: l = 4n$	1.0, 1.7, 3.0, 1.7
				D(0,1)D(0,0)		
$4M_2$	$C2$	0222	3351	D(0,0)D(0,0)	Same as $4M_1$	2.6, 1.7, 1.7, 1.7
				D(0,1)D(0,0)		
$4A_1$†	$C\bar{1}$	$002\bar{2}$	1113	D(0,−1)D(0,1)	Same as $4M_1$	1.0, 0.9, 1.7, 3.3
				D(0,0)D(0,0)		
$4M_3$	$C2/c$	$2\bar{2}\bar{2}2$	3531	D(0,0)D(0,1)	$k = 3n: l = 4n$	2.0, 2.45, 0.0, 2.45
				D(0,1)D(0,0)	$k \neq 3n: l \neq 4n + 2$	

† Labelled 4Tc8 in Ross *et al.* (1966).

8. Discussion

The analysis of the PID of mica polytypes is a powerful method to solve the stacking sequence of these silicates. It can be applied to polytypes of very long period, which could not be solved or would require very complex solution strategies (*e.g.* Kogure & Nespolo, 1999*a*). In spite of the fact that the difference between the PID of polytypes with only slightly different stacking sequences is small, Kogure & Nespolo (1999*a*) have shown that this minimal difference was still sufficient to determine the stacking sequence of a well crystallized 36-layer polytype, *i.e.* the longest mica polytype reported to date. For long-period polytypes, the quality of the crystal might, in principle, become critical, but even in the worst cases PID analysis drastically reduces the number of stacking candidates.

Since PID is the Fourier transform of the stacking vectors giving the relative displacements between TS layers, it is defined in the homo-octahedral approximation. The presence of M2 layers is in principle revealed by a structure refinement.

The calculation of the PID function starting from RTW symbols is accomplished by a computer program (*PTST*98) written in Fortran V, which can be obtained upon request from the correspondence author. Application of the program has been exemplified by Kogure & Nespolo (1999*a*).

8.1. *A preliminary analysis to the application of PID*

The analysis of the geometry of the diffraction pattern should precede the PID analysis, since it offers important preliminary information, which can be summarized as follows.

(i) An analysis of the diffraction-pattern geometry is of particular importance in the case of (suspected) polytypes belonging to *Series* > 0, when twinning may be present (Nespolo, Takeda & Ferraris, 1997; Nespolo, Takeda, Ferraris & Kogure, 1997; Nespolo, 1999).

(ii) The number of reflections along reciprocal-lattice rows corresponding to family reflections of the threefold family structure unequivocally indicate if a mica poly-type is an OD subfamily A, OD subfamily B or mixed-rotation polytype.

(iii) The possibility exists of finding the same PID for polytypes with a different lattice; this is the case for 2O (C_1 setting) and 2M_2 (^{b}F setting) polytypes, which have identical TS symbols (and thus the same PID).

(iv) As shown by Nespolo (1999), only in the ^{a}F settings are the family reflections for *Series* 0 polytypes identical, while this is not true in other settings.

(v) Special attention has to be paid in the case of triclinic polytypes belonging to *Class b*, which admits three equivalent orientations, related by $2n \times 60°$ rotations around $\mathbf{c}^*$. Z symbols and TS symbols are different for the three orientations but they describe three equivalent orientations of the structural model. PID values expressed for a given reciprocal-lattice row in a certain orientation of the structural model correspond to a different row in another orientation. Since these rows are related by $2n \times 60°$ rotations around $\mathbf{c}^*$, for *Series* 0 polytypes the corresponding PID values are in their turn related by equation (17) or (19). For *Series* > 0 polytypes, the comparison requires more attention. In this case, the c axis of the $^{(3^n, a; 3^n, b)}$F setting is displaced by $1/3^n$ for each layer and the length of the axis displacement is a submultiple of the layer stagger; therefore, the origin of the PID is not the same in the three orientations of the structural model. In Table 14, the example of the 3A_1 polytype is presented. The existence of a similar ambiguity in chlorite was reported by Brindley *et al.* (1950).

8.2. *Comparison with previous results*

Comparison of the general results of the present research with previous partial reports reveals some errors.

Ross *et al.* (1966) gave partial reflection conditions for polytypes with up to four layers (see their Table 2). However, the possible ambiguities of the axial setting choice were not recognized and different settings were used to index different polytypes (four different kinds of settings for $2M_1, 3M_1, 4M_9, 4A_2, 4A_9$ and $4A_{10}$ polytypes;

Table 10. *Symbols, reflection conditions and PID values for mixed-rotation Series 0 Class a polytypes (^{a}F setting)*

Polytype	Space-group type	RTW	Z	TS	Reflection conditions	PID 02l	11l	−11l
$4M_4$	$C2/m$	0033	6663	D*(−1,0)D*(1,0)T*(0,0)T(0,0)	$h=3n$: $l=4n$	4.0, 0.0, 0.0, 0.0	1.0, 3.3, 1.7, 0.9	1.0, 0.9, 1.7, 3.3
$4M_5$	$C2$	1122	2346	T*(−1,−1)T(−1,−1)D(1,0)D*(0,0)	$h=3n, k=3n$: $l=4n$ $h=3n, k\neq3n$: $l\neq4n+2$	2.0, 2.45, 0.0, 2.45	2.6, 1.7, 1.7, 1.7	2.6, 1.7, 1.7, 1.7
$4A_2$	$C\bar{1}$	1$\bar{1}\bar{1}$2	6164	T*(−1,0)T(−1,−1)D*(1,−1)D*(0,0)	$h=3n, k=3n$: $l=4n$ $h=3n, k\neq3n$: $l\neq4n+2$ $h\neq3n, k=3n-h$: $l=2n$	2.0, 2.45, 0.0, 2.45	1.0, 3.3, 1.7, 0.9	2.0, 0.0, 3.5, 0.0
$4A_3$	$C1$	1$\bar{3}\bar{2}$2	2364	T*(−1,−1)T(−1,−1)D*(1,−1)D*(0,0)	$h=3n, k=3n$: $l=4n$ h (mod 3) = k (mod 3) ≠ $3n$: $l\neq4n+2$	2.6, 1.7, 1.7, 1.7	2.0, 2.45, 0.0, 2.45	2.6, 1.7, 1.7, 1.7
$4A_4$	$C1$	0213	2245	D*(−1,−1)D*(1,1)T*(0,−1)T(0,0)	$h=3n, k=3n$: $l=4n$	1.0, 1.7, 3.0, 1.7	1.0, 0.9, 1.7, 3.3	2.6, 1.7, 1.7, 1.7
$4A_5$	$C1$	0132	6614	D*(−1,0)T*(1,0)T(1,−1)D*(0,0)	Same as $4A_4$	2.6, 1.7, 1.7, 1.7	1.0, 3.3, 1.7, 0.9	1.0, 1.7, 3.0, 1.7
$4A_{11}$	$C1$	01$\bar{1}\bar{2}$	4456	D*(−1,1)T*(1,−1)T(1,0)D*(0,0)	Same as $4A_4$	1.0, 3.3, 1.7, 0.9	2.6, 1.7, 1.7, 1.7	1.0, 1.7, 3.0, 1.7
$4A_8$†	$C\bar{1}$	$\bar{2}\bar{2}$33	2425	D*(−1,−1)D*(1,0)T*(0,−1)T(0,0)	$h=3n, k=3n$: $l=4n$ $h=3n, k\neq3n$: $l=2n$ $h\neq3n, k=3n-h$: $l\neq4n+2$	2.0, 0.0, 3.5, 0.0	1.0, 0.9, 1.7, 3.3	2.0, 2.45, 0.0, 2.45
$4A_9$	$C\bar{1}$	1$\bar{2}\bar{2}\bar{1}$	1262	T(0,−1)D*(−1,1)D*(1,1)T*(0,0)	$h=3n, k=3n$: $l=4n$ h (mod 3) = k (mod 3) ≠ $3n$: $l=2n$ $h\neq3n, k=3n-h$: $l\neq4n+2$	1.0, 0.9, 1.7, 3.3	2.0, 0.0, 3.5, 0.0	2.0, 2.45, 0.0, 2.45
$4A_{10}$	$C\bar{1}$	00$\bar{1}\bar{1}$	2223	D*(−1,−1)D*(1,1)T*(0,0)T(0,0)	$h+k=3n$: $l=4n$	1.0, 0.9, 1.7, 3.3	1.0, 0.9, 1.7, 3.3	4.0, 0.0, 0.0, 0.0

† Labelled $4Tc_1$ in Ross *et al.* (1966).

Table 11. *Symbols, reflection conditions and PID values for subfamily B Series 0 Class b polytypes (^{b}F setting)*

Polytype	Space-group type	RTW	Z	TS	Reflection conditions	PID 20l	11l	−11l
$2M_2$	$C2/c$	1$\bar{1}$	45	T(−1,0)T*(0,0)	$k=3n$: $l=2n$	2.0, 0.0	1.0, 1.7	1.0, 1.7
$4M_9$	$C2$	1131	4563	T*(1,−1)T(0,1)T*(1,−1)T(0,0)	$h=3n, k=3n$: $l=4n$ $h=3n, k\neq3n$: $l=2n$	1.0, 1.7, 3.0, 1.7	2.6, 1.7, 1.7, 1.7	2.6, 1.7, 1.7, 1.7
$4A_6$	$C\bar{1}$	1$\bar{1}$33	4541	T*(1,−1)T(0,1)T*(1,0)T(0,0)	$h=3n, k=3n$: $l=4n$ $h=3n, k\neq3n$: $l=2n$ h (mod 3) = k (mod 3) ≠ $3n$: $l\neq4n+2$	1.0, 0.9, 1.7, 3.3	2.0, 2.45, 0.0, 2.45	1.0, 3.3, 1.7, 0.9

Table 12. *Symbols, reflection conditions and PID values for mixed-rotation Series 0 Class b polytypes (^bF setting)*

Polytype	Space-group type	RTW	Z	TS	Reflection conditions	PID 20l	PID 11l	PID −11l
$4M_8$	C2/c	010$\bar{1}$	1122	D(−1,0)T(1,0)D*(−1,0)T*(0,0)	$k = 3n$: $l = 4n$	4.0, 0.0, 0.0, 0.0	1.0, 1.7, 3.0, 1.7	1.0, 1.7, 3.0, 1.7
$4M_{10}$	Cc	121$\bar{1}\bar{2}$	3465	T(−1,1)D*(0,0)T*(1,1)D(0,0)	$h = 3n, k = 3n$: $l = 4n$	2.0, 0.0, 3.5, 0.0	2.6, 1.7, 1.7, 1.7	2.6, 1.7, 1.7, 1.7
$4M_{11}$	C2	1$\bar{2}$3$\bar{2}$	4536	T*(1, −1)D(0,1)T(−1, −1)D*(0,0)	$h \neq 3n, k = 3n$: $l = 2n$; $h = 3n, k = 3n$: $l = 4n$	1.0, 1.7, 3.0, 1.7	2.0, 2.45, 0.0, 2.45	2.0, 2.45, 0.0, 2.45
$4A_7$	C1	0123	4451	D*(1, −1)T*(−1,1)D(1,0)T(0,0)	$h \neq 3n, k \neq 3n$: $l \neq 4n + 2$; $h = 3n, k = 3n$: $l = 4n$	1.0, 0.9, 1.7, 3.3	2.6, 1.7, 1.7, 1.7	1.0, 0.3.3, 1.7, 0.9

for $3A_2$ polytype; for $4A_6$ polytype; and for $4M_8$ polytype) or different planes of the same polytype ($3A_1$, $4M_1$, $4M_2$, $4M_3$ and $4A_8$). Besides, as shown by Nespolo & Kogure (1998), for the $3T$ polytype a monoclinic setting was chosen, having an inclined a^* axis parallel to that of the $2M_1$ polytype. Finally, the partial reflection conditions given for $4O_2$, $4M_6$, $4M_9$, $4A_2$, $4A_6$, $4A_8$ and $4A_9$ are correct only for h and/or $k \neq 0 \, (\text{mod} \, 3)$. The reflection conditions analysed for one or two planes only and not for the whole reciprocal lattice erroneously led to $4M_1$, $4M_2$ and $4M_3$ being considered as indistinguishable. Actually, the last one can be differentiated from the previous two by means of the reflection conditions in the (hhl) plane, as shown by Zhukhlistov *et al.* (1988, 1990).† The same remark can be made for $4A_3$, $4A_4$ and $4A_5$ polytypes: the first one can be distinguished from the other two by looking at the geometry of the (hhl) plane (Tables 9 and 10).

Takeda & Ross (1995) gave the reflection conditions that are part of the PID information for the 26 4-layer polytypes (see their Table 6) and the computed PID values for several subfamily A polytypes belonging to the three $1M$, $2M_1$ and $3T$ structural series.‡ However, since the structural model orientation was not taken into account, a few mistakes appeared in their Table 6. The reflection conditions for $4O_3$ and $4M_8$ polytypes are given for $(hhl) - (\bar{h}hl)$ planes instead of for the $(0kl)$ plane. The reflection conditions for the $4O_4$ polytype in the $(hhl) - (\bar{h}hl)$ planes have not been given, while those in the $(0kl)$ plane of the $4M_9$ polytype should not be present. The space-group type of the $4M_{10}$ polytype has been misprinted as $C2/c$ instead of Cc [the same misprint occurs in the papers by Ross *et al.* (1966) and Takeda (1971)]. Another misprint is in their Table 4, where the third value of the PID for the $(hhl) - (\bar{h}hl)$ planes of the $3M_2$ polytype is 2.5 and not 0.9. On the basis of the generalized notation introduced by Nespolo *et al.* (1998), all the axial settings labelled $1M$ should be changed into ^aF, and those labelled $3M_1$ into $^{3,a}F$; the settings $3Tc_1$ and $9Tc_1$ become $^{3,b}F$ and $^{9,b}F$ if the axial exchange $a \leftrightarrow b$ is accomplished. All polytypes belonging to structural series $3T$ listed in Table 9 of Takeda & Ross (1995) belong to *Class a* and the axial setting in which PID is expressed is ^aF.

Polytype $3A_1$ belongs to subfamily A but it is a *Series 1 Class b* polytype. It is described by M layers in even orientation but, being a triclinic polytype, three orientations of the structural model are possible. Among

---

† The orthohexagonal 12-layer indexing given by Zhukhlistov *et al.* (1988, 1990) corresponds to the 4-layer monoclinic indexing shown in Table 9 of the present paper if the condition of integrality of monoclinic indices is taken into account.

‡ The definition of 'series' in Takeda & Ross (1995) corresponds to that of 'structural series' in Baronnet (1978): it indicates the short-period polytype that is thought to have given origin to the long-period ones. This should not be confused with the definition of *Series* by Nespolo *et al.* (1998), which has a geometrical meaning.

Table 13. *Symbols, reflection conditions and PID values for mixed-rotation Series 1 Class a non-orthogonal polytypes* ($^{a}S \equiv {}^{3a}F$ *setting*)

Polytype	Space-group type	RTW	Z	TS	Reflection conditions	PID 02l	11l	−11l
$3M_1$	$C2/m$	033	336	D(−2,0)T(−4,0)T*(0,0)	$h = 3n$: $l = 3n − h/3$	3.0, 0.0, 0.0	1.3, 2.5, 0.9	1.3, 0.9, 2.5
$3M_2$	$C2$	11$\bar{2}$	561	T(−2,1)T*(2,1)D(0,0)	$h = 3n$, $k = 3n$: $l = 3n − h/3$	1.7, 1.7, 1.7	0.9, 1.3, 2.5	0.9, 2.5, 1.3
$3A_2$	$C\bar{1}$	01$\bar{1}$	112	D(−2,−1)T(−4,1)T*(0,0)	$h = 3n$: $l = 3n + k − h/3$	0.0, 0.0, 3.0	0.9, 1.3, 2.5	2.5, 1.3, 0.9
$3A_3$	$C1$	123	235	T*(4,−1)D(2,−1)T(0,0)	Same as $3M_2$	1.7, 1.7, 1.7	2.5, 0.9, 1.3	1.3, 0.9, 2.5

Table 14. *Symbols, reflection conditions and PID values for subfamily A Series 1 Class b non-orthogonal polytype* ($^{b}S \equiv {}^{3b}F$ *setting*)

Polytype	Space-group type	RTW	Z	TS	Reflection conditions	PID 20l	11l	−11l
$3A_1$	$C\bar{1}$	02$\bar{2}$	662	D*(1,1)D*(−1,2)D*(0,0)	$h = 3n$: $l = 3n − h/3 − k$	1.3, 2.5, 0.9	0.9, 2.5, 1.3	1.3, 2.5, 0.9
			224	D*(1,−2)D*(−1,−4)D*(0,0)		0.9, 1.3, 2.5	2.5, 1.3, 0.9	0.9, 1.3, 2.5
			446	D*(1,4)D*(−1,−1)D*(0,0)		2.5, 0.9, 1.3	1.3, 0.9, 2.5	2.5, 0.9, 1.3

these, one corresponds to Z symbols 2 and 4, as polytype $2M_1$. The period along $\mathbf{c}^*$ of an N-layer polytype is $c_N^* = Nc_1^*$ (Nespolo *et al.*, 1998). The appearance of $(h0l)$ and $(h.3h.l)$ planes (C_1 setting), containing only family reflections, is the same for $2M_1$ and $3A_1$ polytypes (Borutskiy *et al.*, 1987).† However, this identity does not hold for other planes, where non-family reflections appear and no common axial setting can be found, since polytypes belonging to a *Series* cannot be indexed in the monoclinic setting of any polytype belonging to another *Series*.

We are deeply indebted to Professor Boris B. Zvyagin (IGEM, RAS, Moscow), Professor Slavomil Ďurovič (Slovak Academy of Sciences, Bratislava) and Professor Jillian F. Banfield (University of Wisconsin–Madison) for several fundamental discussions and for critical reading of the manuscript. We thank Professor Yoshio Takéuchi (Nihon University, Tokyo), Professor Ryoichi Sadanaga (Japan Academy), Dr Malcom Ross (US Geological Service), Professor Stefano Merlino (University of Pisa), Professor Takeo Matsumoto (University of Kanazawa) and Dr Akiji Yamamoto (NIRIM, Tsukuba) for valuable discussions, and Professor D. Yu. Pushcharovsky (Moscow State University) for sending consultation material. MN is also indebted to Professor Masamichi Miyamoto (University of Tokyo) and Professor Yasunari Watanabe (Teikyo Heisei University) for their constant encouragement. This research has been partly developed during a Doctoral Program (MN) supported by the Japanese Ministry of Education, Science and Culture.

References

Andreeva, N. S. (1962). *Sov. Phys. Crystallogr.* **6**, 419–422.

Arnold, H. (1996). *International Tables for Crystallography*, Vol. A, edited by Theo Hahn, part 5. Dordrecht: Kluwer Academic Publishers.

Backhaus, K.-O. (1983). *Cryst. Res. Techn.* **18**, 1253–1260.

Backhaus, K.-O. & Ďurovič, S. (1984). *Clays Clay Miner.* **32**, 453–463.

Bailey, S. W. & Christie, O. H. J. (1978). *Am. Mineral.* **63**, 203–204.

Baronnet, A. (1978). *Progress in Crystal Growth and Characterics*, Vol. 1, pp. 151–211. Oxford: Pergamon Press.

Belov, N. V. (1949). *Mineralog. Sb. L'vovsk. Geol. Obshchestvo pri L'vovsk. Gos. Univ.* **3**, 29–40. (In Russian.)

Borutskiy, B. Y., Soboleva, S. V. & Golovanova, T. I. (1987). *Dokl. Acad. Sci. USSR Earth Sci. Sect.* **294**, 141–143.

Brindley, G. W., Oughton, B. M. & Robinson, K. (1950). *Acta Cryst.* **3**, 408–416.

Catti, M., Ferraris, G. & Ivaldi, G. (1989). *Eur. J. Miner.* **1**, 625–632.

Černý, P., Rieder, M. & Povondra, P. (1970). *Lithos*, **3**, 319–325.

Dekeyser, W. & Amelinckx, S. (1953). *C. R. XIX Session Congr. Geol. Intern.* Comité International pour l'Étude des Argiles, Alger, fasc. XVIII, pp. 23–33.

Donnay, G., Morimoto, N., Takeda, H. & Donnay, J. D. H. (1964). *Acta Cryst.* **17**, 1369–1373.

Dornberger-Schiff, K. (1959). *Acta Cryst.* **12**, 173.

Dornberger-Schiff, K. (1964). *Grundzüge einer Theorie von OD-Strukturen aus Schichten. Abh. Dtsch. Akad. Wiss. Berlin, Kl. Chem.* No 3.

Dornberger-Schiff, K., Backhaus, K.-O. & Ďurovič, S. (1982). *Clays Clay Miner.* **30**, 364–374.

---

† Borutskiy *et al.* (1987) gave odd Z symbols for the $3A_1$ polytype, namely 113, while it must be described by even Z symbols.

Dornberger-Schiff, K. & Farkas-Jahnke, M. (1970). *Acta Cryst.* A**26**, 24–34.

Ďurovič, S. (1979). *Krist. Tech.* **14**, 1047–1053.

Ďurovič, S. (1992). *International Tables for Crystallography*, Vol. C, edited by A. C. J. Wilson, Section 9.2.2. Dordrecht: Kluwer Academic Publishers.

Ďurovič, S. (1994*a*). *Ceramics-Silikáty*, **38**, 81–84.

Ďurovič, S. (1994*b*). *Aperiodic '94. Proceedings of the International Conference on Aperiodic Crystals*, edited by G. Chapuis & W. Paciorek, pp. 595–599. Singapore: World Scientific.

Ďurovič, S. (1997). *Modular Aspects of Minerals/EMU Notes in Mineralogy*, Vol. 1, edited by S. Merlino, pp. 1–28. Budapest: Eötvös University Press.

Ďurovič, S. & Weiss, Z. (1986). *Bull. Minéral.* **109**, 15–29.

Ďurovič, S., Weiss, Z. & Backhaus, K.-O. (1984). *Clays Clay Miner.* **32**, 454–474.

D'yakonov, Yu. S. (1962). *Sov. Phys. Crystallogr.* **6**, 499–500.

D'yakonov, Yu. S. (1963). *Sov. Phys. Crystallogr.* **6**, 715–717.

Farkas-Jahnke, M. (1966). *Acta Cryst.* **21** A173.

Farkas-Jahnke, M. & Dornberger-Schiff, K. (1970). *Acta Cryst.* A**26**, 35–41.

Fichtner-Schmittler, H. (1979). *Krist. Tech.* **14**, 1079–1088.

Filut, M. A., Rule, A. C. & Bailey, S. W. (1985). *Am. Mineral.* **70**, 1298–1308.

Giuseppetti, G. & Tadini, C. (1972). *Tschermaks Mineral. Petrogr. Mitt.* **18**, 169–184.

Guggenheim, S. (1981). *Am. Mineral.* **66**, 1221–1232.

Guggenheim, S. & Bailey, S. W. (1975). *Am. Mineral.* **60**, 1023–1029.

Guggenheim, S. & Bailey, S. W. (1977). *Am. Mineral.* **62**, 1158–1167.

Guggenheim, S. & Bailey, S. W. (1978). *Am. Mineral.* **63**, 186–187.

Guinier, A., Bokij, G. B., Boll-Dornberger, K., Cowley, J. M., Ďurovič, S., Jagodzinski, H., Khrisna, P., de Wolff, P. M., Zvyagin, B. B., Cox, D. E., Goodman, P., Hahn, Th., Kuchitsu, K. & Abrahams, S. C. (1984). *Acta Cryst.* A**40**, 399–404.

Hahn, Th. & Vos, A. (1996). *International Tables for Crystallography*, Vol. A, edited by Th. Hahn, Section 2.13. Dordrecht: Kluwer Academic Publishers.

Kogure, T. (1997). *Mineral. J.* **19**, 155–164.

Kogure, T. & Nespolo, M. (1999*a*). *Acta Cryst.* B. In the press.

Kogure, T. & Nespolo, M. (1999*b*). *Clays Clay Miner.* Submitted.

Lipson, H. & Taylor, C. A. (1958) *Fourier Transforms and X-ray Diffraction.* London: Bell.

Matsumoto, T. & Wondratschek, H. (1979). *Z. Kristallogr.* **150**, 181–198.

Matsumoto, T. & Wondratschek, H. (1987). *Z. Kristallogr.* **189**, 7–30.

Merlino, S. (1990). *Period. Mineral.* **59**, 69–92.

Merlino, S. (1997). *Modular Aspects of Minerals/EMU Notes in Mineralogy*, Vol. 1, edited by S. Merlino, pp. 29–54. Budapest: Eötvös University Press.

Nespolo, M. (1998). Doctoral dissertation, University of Tokyo, Japan.

Nespolo, M. (1999). *Mineral. J.* **21**. In the press

Nespolo, M. & Kogure, T. (1998). *Z. Kristallogr.* **213**, 4–12.

Nespolo, M., Takeda, H. & Ferraris, G. (1997). *Modular Aspects of Minerals/EMU Notes in Mineralogy*, Vol. 1, edited by S. Merlino, pp. 81–118. Budapest: Eötvös University Press.

Nespolo, M., Takeda, H. & Ferraris, G. (1998). *Acta Cryst.* A**54**, 348–356.

Nespolo, M., Takeda, H., Ferraris, G. & Kogure, T. (1997). *Mineral. J.* **19**, 173–186.

Ohta, T., Takeda, H. & Takéuchi, Y. (1982). *Am. Mineral.* **67**, 298–310.

Pabst, A. (1959). *Z. Kristallogr.* **112**, 53–59.

Pabst, A. (1961). *Z. Kristallogr.* **115**, 307–309.

Pauling, L. (1930). *Proc. Natl Acad. Sci. USA*, **16**, 123–129.

Pavese, A., Ferraris, G., Ivaldi, G., Pischedda, V. & Nespolo, M. (1998). 17th IMA General Meeting, Toronto, Canada. Abstract A102.

Pavese, A., Ferraris, G., Prencipe, M. & Ibberson, R. (1997). *Eur. J. Miner.* **9**, 1183–1190.

Radoslovich, E. W. (1961). *Nature (London)*, **191**, 67–68.

Ramsdell, L. S. (1947). *Am. Mineral.* **32**, 64–82.

Rieder, M. (1968). *Science*, **160**, 1338–1340.

Rieder, M., Cavazzini, G., D'Yakonov, Yu. S., Frank-Kamenetskii, V. A., Gottardi, G., Guggenheim, S., Koval', P. V., Müller. G., Neiva, A. M. R., Radoslovich, E. W., Robert, J. L., Sassi, F. P., Takeda, H., Weiss, Z. & Wones, D. R. (1998). *Can. Mineral.* **36**, 905–912.

Ross, M., Takeda, H. & Wones, D. R. (1966). *Science*, **151**, 191–193.

Rule, A. C., Bailey, S. W., Livi, K. J. T. & Veblen, D. R. (1987). *Am. Mineral.* **72**, 1163–1169.

Rumanova, I. M. & Belov, N. V. (1961). *Sov. Phys. Crystallogr.* **5**, 215–217.

Sadanaga, R. & Takeda, H. (1964). *Mineral. J.* **4**, 159–171.

Sadanaga, R. & Takeda, H. (1969). *J. Miner. Soc. Jpn*, **9**, 177–184. (In Japanese.)

Smith, J. V. & Yoder, H. S. (1956). *Mineral. Mag.* **31**, 209–235.

Takeda, H. (1961). Doctoral dissertation, University of Tokyo, Japan.

Takeda, H. (1967). *Acta Cryst.* **22**, 845–853.

Takeda, H. (1971). *Am. Mineral.* **56**, 1042–1056.

Takeda, H. & Burnham, C. W. (1969). *Mineral. J.* **6**, 102–109.

Takeda, H. & Donnay, J. D. H. (1965). Am. Crystallogr. Assoc. Winter Meeting, Program and Abstracts, pp. 23–24.

Takeda, H., Haga, N. & Sadanaga, R. (1971). *Mineral. J.* **6**, 203–215.

Takeda, H. & Horiuchi, H. (1971). *J. Miner. Soc. Jpn*, **10**, 283–295. (In Japanese.)

Takeda, H. & Mori, N. (1970). *J. Crystallogr. Soc. Jpn*, **12**, 231–248. (In Japanese.)

Takeda, H. & Morosin, B. (1975). *Acta Cryst.* B**31**, 2444–2452.

Takeda, H. & Ross, M. (1995). *Am. Mineral.* **80**, 715–724.

Takeda, H. & Sadanaga, R. (1969). *Mineral. J.* **5**, 434–449.

Takéuchi, Y. (1971). *J. Miner. Soc. Jpn*, **10**, Spec. Issue No. 2, 87–99. (In Japanese.)

Takéuchi, Y. & Haga, N. (1971). *Miner. Soc. Jpn Spec. Pap.* **1** , 74–87. (Proc. IMA-IAGOD Meetings '70, IMA Vol.)

Takéuchi, Y. & Sadanaga, R. (1959). *Acta Cryst.* **12**, 945–946.

Templeton, D. H. (1956). *Acta Cryst.* **9**, 199–200.

Tokonami, M. (1966). *Mineral. J.* **4**, 401–423.

Tokonami, M. & Hosoya, S. (1965). *Acta Cryst.* **18**, 908–916.

Weiss, Z. & Wiewióra, A. (1986). *Clays Clay Miner.* **34**, 53–68.

Wondratschek, H. (1976). *Z. Kristallogr.* **143**, 460–470.

Zhukhlistov, A. P., Zvyagin, B. B. & Pavlishin, V. I. (1988). *Z. Kristallogr.* **185**, 624.

Zhukhlistov, A. P., Zvyagin, B. B. & Pavlishin, V. I. (1990). *Sov. Phys. Crystallogr.* **35**, 232–236.

Zhukhlistov, A. P., Zvyagin, B. B., Soboleva, S. V. & Fedotov, A. F. (1973). *Clays Clay Miner.* **21**, 465–470.

Zvyagin, B. B. (1962). *Sov. Phys. Crystallogr.* **6**, 571–580.

Zvyagin, B. B. (1967). *Electron Diffraction Analysis of Clay Mineral Structures.* New York: Plenum Press.

Zvyagin, B. B. (1974). 2nd Eur. Crystallogr. Meet. Collect. Abstracts, Keszthely, pp. 162–164.

Zvyagin, B. B. (1985). *Sov. Phys. Crystallogr.* **32**, 394–399.

Zvyagin, B. B. (1988). *Comput. Math. Appl.* **16**, 569–591.

Zvyagin, B. B. (1997). *Modular Aspects of Minerals/EMU Notes in Mineralogy*, Vol. 1, edited by S. Merlino, pp. 345–372. Budapest: Eötvös University Press.

Zvyagin, B. B., Rabotnov, V. T., Sidorenko, O. V. & Kotel'nikov, D. D. (1985). *Izv. Akad. Nauk SSSR Ser. Geol.* **5**, 121–124. (In Russian.)

Zvyagin, B. B., Vrublevskaya, Z. V., Zhukhlistov, A. P., Sidorenko, O. V., Soboleva, S. V. & Fedotov, A. F. (1979). *High-Voltage Electron Diffraction in the Study of Layered Minerals.* Moscow: Nauka. (In Russian.)